

Carbon tri-interstitial defect: A model for the D_{II} centerChao Jiang,^{*} Dane Morgan,[†] and Izabela Szlufarska[‡]*Department of Materials Science and Engineering, University of Wisconsin, Madison, WI 53706, USA*

(Received 26 July 2012; published 31 October 2012)

Using a combination of random configuration sampling, molecular dynamics simulated annealing with empirical potential, and ensuing structural refinement by first-principles density functional calculations, we perform an extensive ground-state search for the most stable configurations of small carbon interstitial clusters in SiC. Our search reveals a “magic” cluster number of three atoms, where the formation energy per interstitial shows a distinct minimum. A carbon tri-interstitial cluster with trigonal C_{3v} symmetry is discovered, in which all carbon atoms are fourfold coordinated. In addition to its special thermodynamic stability, its localized vibrational modes are also in a very good agreement with the experimental photoluminescence spectra of the D_{II} center in both 3C- and 4H-SiC. The D_{II} center is one of the most persistent defects in SiC, and we propose that the discovered carbon tri-interstitial is responsible for this center.

DOI: [10.1103/PhysRevB.86.144118](https://doi.org/10.1103/PhysRevB.86.144118)

PACS number(s): 61.72.jj, 63.20.Pw, 78.55.-m

I. INTRODUCTION

Silicon carbide (SiC) is a promising semiconductor for high temperature, high power, and high frequency devices due to its wide band gap, high thermal conductivity, and high electric field breakdown strength.^{1,2} During dopant implantation, lattice defects (e.g., vacancies and interstitials) are inevitably created, which can adversely affect the optical and electrical properties of devices.³ Therefore, high temperature annealing is necessarily performed to eliminate the implantation damage. Interestingly, in SiC, several defects are exceptionally stable against heat treatment, and the photoluminescence (PL) center D_{II} is one such example. The D_{II} center has been observed in both ion-implanted⁴⁻⁶ and electron-irradiated⁷ SiC samples and persists even after annealing at 1973 K. Its existence is independent of implanted species or SiC polytype, indicating that it is an intrinsic defect. Furthermore, the high annealing temperature required for the formation of the D_{II} center (1473–1573 K^{4,7}) suggests that it is due to a defect complex.

A fundamental understanding of the microscopic origin of the D_{II} center is critical for further improvement of the fabrication and performance of SiC devices. Based on the observation that the D_{II} center exhibits five localized vibrational modes (LVMs) above the SiC bulk phonon spectrum (up to ~ 120 meV), Patrick and Choyke proposed a carbon di-interstitial model for the D_{II} center.⁴ Later Mattausch *et al.*⁸⁻¹⁰ performed density functional theory (DFT) calculations of vibrational spectra of various defect complexes and suggested di-carbon antisite as a possible building block of the D_{II} center, where two C atoms occupy a vacant Si site and form a dumbbell along the $\langle 001 \rangle$ direction. Gali *et al.*¹¹ further speculated that a di-carbon antisite pair can be the D_{II} center. However, to date, a model that can satisfactorily explain all features of the D_{II} center is yet to be found.^{9,10,12} In particular, according to PL experiments,^{4,7} the D_{II} center exhibits five LVMs in 3C-SiC and 10 LVMs in 4H-SiC—properties that have not been successfully reproduced by any of the existing defect models.

In this paper, we present findings of the ground-state (GS) configurations of small carbon interstitial clusters in cubic 3C-SiC obtained using classical molecular dynamics (MD)

simulations combined with first-principles DFT calculations. Our search reveals a carbon tri-interstitial cluster that is energetically remarkably stable. Furthermore, its calculated LVMs are in a very good agreement with the experimental PL spectra of the D_{II} center in both 3C- and 4H-SiC. We therefore propose this newly discovered defect as a model for the D_{II} center in SiC.

II. METHODOLOGY

The determination of GS configuration of a cluster of atoms can be quite challenging due to the existence of numerous local minima on the potential energy surface (PES), especially when the cluster size is large.¹³⁻¹⁵ When the cluster is embedded in a crystal as a defect, an additional complexity arises due to the electronic and elastic interactions of this cluster with the underlying lattice, in which interactions can be long range in nature. Furthermore, in SiC, when transitions between different defect cluster configurations involve the breaking of strong covalent bonds, the associated energy barriers can be very high, and, therefore, such transitions are unlikely to be observed in MD simulations due to their inherent time-scale limitations. In this study, we overcome these difficulties by using a combination of the random structure searching^{16,17} and MD simulated annealing¹⁴ techniques. To allow adequate sampling of the PES, we randomly generate many defect cluster configurations by placing C-C split interstitials in close proximity to each other within a perfect 216-atom cubic SiC supercell. Such a large supercell is necessary to prevent unphysical interactions between a defect cluster and its periodic images. The orientations and relative positions of these dumbbells are chosen randomly. To avoid being trapped in local minima, we further subject these random initial configurations to MD simulated annealing using a recently developed environment-dependent interatomic potential (EDIP) for SiC,¹⁸ which we have implemented in Large-scale Atomic/Molecular Massively Parallel Simulator (LAMMPS).¹⁹ The EDIP potential is chosen since it provides a good description of energetics of point and extended defects,^{18,20} which is particularly important for our study. Simulations are performed in the canonical (constant temperature, constant volume) ensemble with a Nose-Hoover

thermostat for temperature control and a time step of 1 fs. The system is first annealed at a high starting temperature of 2000 K for 10 ps and then gradually cooled down to 300 K over the period of 1 ns. An energy minimization using the conjugate gradient (CG) scheme is performed to obtain the final relaxed configurations.

Our search unveils many distinct defect cluster structures in SiC, the majority of which have not been previously identified. This finding highlights the complexity of the PES of SiC, showing it to be similar in complexity to that found in Si.^{21–23} In fact, due to the presence of two atomic species in SiC, its PES can be much more complicated than pure Si. Although the EDIP potential may not perfectly agree with DFT, it provides a good starting point for ensuing structural refinements. Among the pool of candidate structures from MD simulated annealing, the ones with low formation energies (not necessarily the GS according to EDIP) are further reoptimized using DFT calculations within the local density approximation, as implemented in Vienna *Ab initio* Simulation Package (VASP).²⁴ The electron-ion interactions are described by the projector-augmented wave (PAW) method.²⁵ We use PAW pseudopotentials with valence electron configurations of $2s^2 2p^2$ for C and $3s^2 3p^2$ for Si. The cutoff energy for plane-wave basis sets is set at 500 eV. For Brillouin zone sampling, a $2 \times 2 \times 2$ Monkhorst–Pack k -point mesh is used for the 216-atom supercells. By computing the quantum mechanical Hellmann-Feynman forces, all internal atomic positions are fully optimized using CG method until forces are less than 0.02 eV/\AA .

III. RESULTS AND DISCUSSION

In Table I, we show the DFT calculated binding energies (BEs) of small carbon interstitial clusters (I_n , $n \leq 4$) in both GS and metastable configurations. Comparisons with previous studies^{10,11} are made, when possible. Here BE is defined as the energy required to fully dissociate I_n into n noninteracting C split interstitials in the tilted $\langle 001 \rangle$ configuration.¹⁰ For a given cluster size n , the GS structure corresponds to the one with the highest BE. For I_2 , we find that the GS structure is formed by two C interstitials occupying the bond-center (BC) positions between Si and C atoms, hereinafter referred to as $(C_{BC})_2$ [Fig. 1(a)]. This finding is in agreement with previous studies by Mattausch *et al.*¹⁰ and Gali *et al.*¹¹ A

TABLE I. First-principles calculated BEs of small carbon interstitial clusters in 3C-SiC. Defects in the neutral charge state are considered.

n	Cluster structure	BE (eV per cluster)		
		This study	Ref. 10	Ref. 11
2	$(C_{BC})_2$	5.16	4.8	5.3
	$(C_{sp})_2$	2.81	2.8	2.9
3	$(C_{BC})_3$	9.52	–	–
	$(C_{sp})_3$	5.83	5.8	–
4	$(C_{sp})_4$	12.37	11.5	–
	$[(C_2)_{hex}]_2$	10.09	9.2	–
	Tri-pentagon	10.76	–	–
	Chainlike	10.67	–	–

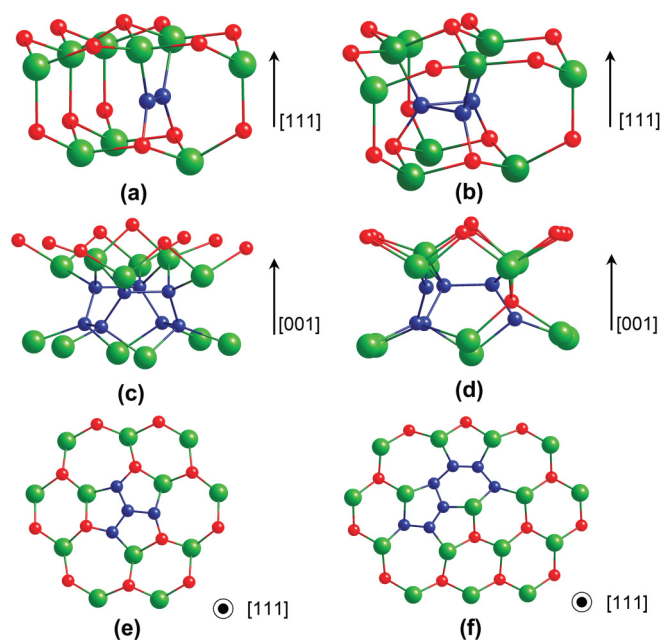


FIG. 1. (Color online) First-principles refined GS structures of small carbon interstitial clusters in 3C-SiC: (a) $(C_{BC})_2$, (b) $(C_{BC})_3$, and (c) $(C_{sp})_4$. The metastable (d) $(C_{sp})_3$, (e) tri-pentagon, and (f) chainlike configurations are also shown. Large and small spheres represent Si and C atoms, respectively.

particularly interesting result of our study is the discovery of a tri-interstitial cluster configuration in C_{3v} symmetry with the C_3 rotation axis along the $\langle 111 \rangle$ direction ($[0001]$ in 4H-SiC), which is shown in Fig. 1(b); see also supplementary material.²⁶ This structure has been previously unknown. Here, the three C interstitials occupy BC positions (approximately in the middle of the original Si-C bonds) and form an equilateral triangle parallel to the $\{111\}$ plane ($[0001]$ in 4H-SiC). We therefore refer to it as the $(C_{BC})_3$ defect. The C-C distance in the triangle is 1.54 \AA , which is identical to the equilibrium C-C bond length in diamond. Each of the three C atoms in the ring also forms a strong C-C bond with a lattice C atom with a shorter bond length of 1.47 \AA . From Table I, it can be seen that $(C_{BC})_3$ is 3.69 eV more stable than the previously known GS of I_3 , designated as $(C_{sp})_3$,^{10,27} making $(C_{BC})_3$ the new GS of I_3 . As shown in Fig. 1(d), $(C_{sp})_3$ consists of three neighboring C-C $\langle 001 \rangle$ split interstitials tilted towards each other. Interestingly, all atoms in $(C_{BC})_3$ are fourfold coordinated (sp^3 hybridized), while the $(C_{sp})_3$ configuration contains two dangling bonds, which may explain the exceptional stability of the former. For I_4 , our predicted GS structure is identical to the previously known $(C_{sp})_4$ configuration [Fig. 1(c)] predicted by Mattausch *et al.*¹⁰ In addition, we find several previously unidentified metastable structures that are energetically competitive, including a tri-pentagon structure [Fig. 1(e)] and a chainlike structure [Fig. 1(f)], both within the $\{111\}$ plane of SiC. Note that since all bonds in $(C_{BC})_3$ are already saturated, we do not find any energetically favorable I_4 structures by adding another C interstitial to $(C_{BC})_3$. For $n > 4$, the number of local minima on the PES increases rapidly, and the many specific structures are not shown here for brevity.

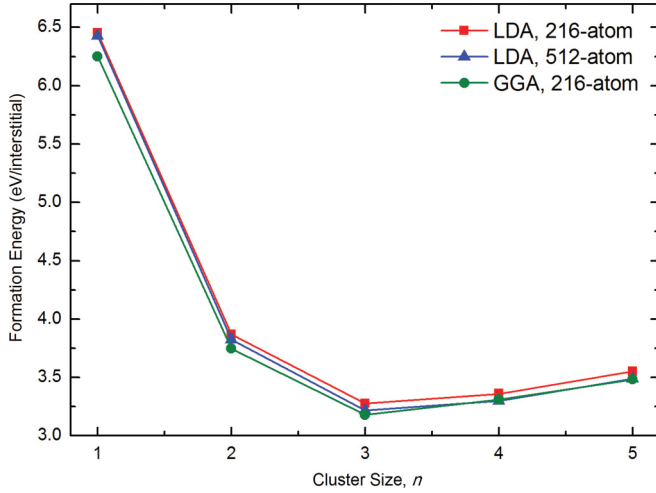


FIG. 2. (Color online) First-principles calculated formation energies (per interstitial) of small carbon interstitial clusters in the neutral charge state as a function of cluster size. Formation energies are given by Eq. (1) in the text.

Figure 2 shows DFT calculated formation energies (per interstitial) of small carbon interstitial clusters (I_n , $n \leq 5$) in their respective GS configurations in 3C-SiC. For all these clusters, our spin-polarized calculations lead to a nonmagnetic state. The defect formation energy is defined as^{28,29}

$$\Delta E_f = E_{\text{defect}} - n_{\text{Si}}\mu_{\text{Si}} - n_{\text{C}}\mu_{\text{C}} + q(\varepsilon_{\text{VBM}} + \Delta\varepsilon_F) \quad (1)$$

where E_{defect} is the total energy of a supercell containing a defect in charge state q . n_i and μ_i denote the number and chemical potential of species i ($i = \text{Si}, \text{C}$), respectively. $\Delta\varepsilon_F$ is the Fermi level relative to ε_{VBM} , the valence band maximum of perfect SiC. The neutral charge state is assumed for all clusters in our study. This assumption is consistent with previous findings for both I_2 and I_4 , whose GS structures are electrically neutral for all values of the Fermi level.²⁷ To ensure that the $(\text{C}_{\text{BC}})_3$ cluster can be treated as neutral,

we have calculated its formation energies in charge states from -3 to $+3$. To overcome the band gap errors inherent in standard DFT functionals, we employ the Heyd-Scuseria-Ernzerhof (HSE06) screened hybrid functional.³⁰ For charged systems, the monopole correction according to Leslie and Gillan³¹ is applied. Our calculations indicate that the $(\text{C}_{\text{BC}})_3$ cluster is neutral ($q = 0$) under most conditions ($\Delta\varepsilon_F > 0.23$ eV), which justifies our focus on its neutral energetics and vibrational modes in this work. For the chemical potentials of pure elements, the C-rich condition is chosen,³² although our conclusions do not depend on such a particular choice. Remarkably, the formation energy per interstitial exhibits a strong minimum at “magic” size $n = 3$, indicating that our newly found $(\text{C}_{\text{BC}})_3$ defect is particularly stable in SiC. Interesting “magic” sizes of defect clusters have also been found in pure Si.^{22,33} To rule out the possibility that such a minimum is a computational artifact, we have performed additional calculations employing larger 512-atom supercells as well as Perdew–Burke–Ernzerhof generalized gradient approximation (GGA).³⁴ We find that the special stability of $(\text{C}_{\text{BC}})_3$ is not due to a particular choice of exchange–correlation functional or supercell size and therefore should represent real physics.

In view of the special stability of $(\text{C}_{\text{BC}})_3$, we further explore the possibility that this defect can be a model for the D_{II} center by calculating its LVMs in both 3C- and 4H-SiC, where experimental PL spectra of the D_{II} center have been reported.^{4,7} One fascinating feature of SiC is its ability to crystallize in many different polytypes, depending on the stacking of Si-C bi-layers. In 3C- and 4H-SiC, the stacking sequences are ABC and ABAC, respectively. In 4H-SiC, two possible $(\text{C}_{\text{BC}})_3$ configurations can exist, depending on whether the defect cluster resides in a cubic (k) or hexagonal (h) bi-layer. In contrast, only the cubic configuration is present in 3C-SiC. Large 216- and 256-atom supercells are used to obtain the LVMs of $(\text{C}_{\text{BC}})_3$ in 3C- and 4H-SiC, respectively. We adopt the defect molecule approximation^{9,10} and constrain our LVM calculations to approximately 22 atoms, including the defect

TABLE II. First-principles calculated LVMs (in meV) of carbon clusters in 3C- and 4H-SiC. The number in the square brackets gives the degeneracy of the corresponding mode. For $(\text{C}_2)_{\text{Si}}$, results for both the high-spin (hs) and low-spin (ls) states are given. Only modes above the bulk spectrum are shown. In the present study, the bulk phonon limit of 3C- and 4H-SiC is calculated to be 118.2 and 117.5 meV, respectively.

Mode	3C						Exp. ^c	4H		
	$(\text{C}_{\text{BC}})_3$	$(\text{C}_2)_{\text{Si}}\text{-hs}$	$(\text{C}_2)_{\text{Si}}\text{-hs}^{\text{a}}$	$(\text{C}_2)_{\text{Si}}\text{-ls}^{\text{a}}$	$[(\text{C}_2)_{\text{Si}}]_2^{\text{a}}$	$[(\text{C}_2)_{\text{Si}}]_2^{\text{b}}$		$(\text{C}_{\text{BC}})_3\text{-}h$	$(\text{C}_{\text{BC}})_3\text{-}k$	Exp. ^d
1	160.4 [2]	173.5	177.5	177.5	169.7	165	164.7	164.8 [2]	159.3 [2]	164.1
2	156.7	141.0 [2]	141.8 [2]	148.3	168.6	163	152.2	160.1	157.0	160.0
3	145.3	121.3	123.2	139.4	139.3	147	146.3	147.7	145.8	156.8
4	135.7			128.5	127.1	132	130.9	135.3	135.7	153.9
5	126.8 [2]			116.4	125.6	121	127.8	127.9 [2]	125.7 [2]	148.7
6					123.3	120				145.9
7										141.9
8										137.1
9										126.9
10										123.8

^aFrom Ref. 9.

^bFrom Ref. 11.

^cFrom Ref. 4.

^dFrom Ref. 7.

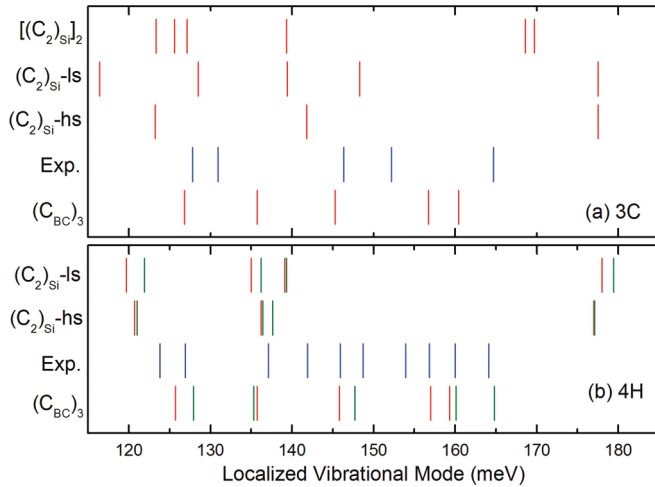


FIG. 3. (Color online) Calculated LVMs of several possible structure models for the D_{II} center in (a) 3C-SiC and (b) 4H-SiC, in comparison with experimental data from Refs. 4 and 7. Results for $(C_2)_{Si}$ and $[(C_2)_{Si}]_2$ are from Ref. 9. Red (dark gray) and green (gray) lines represent LVMs of defect clusters in cubic and hexagonal environments, respectively.

cluster itself and its nearest neighbors, with all other atoms rigidly constrained during such calculations. According to Mattausch *et al.*,⁹ such an approximation only affects the least localized modes that fall close to the bulk phonon spectrum. The vibrational frequencies are obtained from the eigenvalues of the Hessian matrix constructed using central difference method and a small displacement of ± 0.02 Å.

Our calculated LVMs of $(C_{BC})_3$ are summarized in Table II and in Fig. 3, together with those of the previously proposed candidates for the D_{II} center. A group theory analysis reveals that the seven LVMs of $(C_{BC})_3$ consist of three A_1 modes and two doubly degenerate E modes. All seven modes are both Raman and infrared active. For di-carbon antisite $(C_2)_{Si}$ in the high-spin (hs) state, our calculated LVMs agree well with the previous calculations by Mattausch *et al.*^{9,10} reported for the same defect. As was pointed out by Mattausch *et al.*,^{9,10} di-carbon antisite pair $[(C_2)_{Si}]_2$ shows a small splitting of the two highest LVMs, which is not observed experimentally.⁴ In contrast, the two highest LVMs of $(C_{BC})_3$ are found to be degenerate, which is consistent with the aforementioned symmetry of this cluster. As shown in Fig. 4, both modes involve the tilting of the three-atom ring in $(C_{BC})_3$. In one mode, two atoms in the ring move in the same direction,

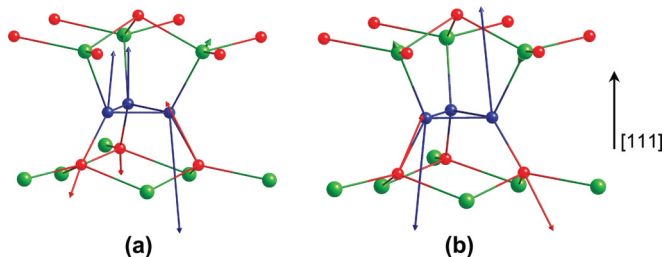


FIG. 4. (Color online) The two highest frequency local vibrational modes of $(C_{BC})_3$ in 3C-SiC. Large and small spheres represent Si and C atoms, respectively. The arrows represent the eigenvectors of the vibrational modes.

with the third atom moving in the opposite direction. In the other mode, one atom remains stationary with the two other atoms oscillating in opposite directions. In 3C-SiC, while both $(C_2)_{Si}$ in the low-spin (ls) state and $(C_{BC})_3$ each produce five LVMs above the bulk continuum compatible with experiments,⁴ the r.m.s. error from experiments is somewhat smaller for $(C_{BC})_3$ (3.6 meV) than for $(C_2)_{Si}$ -ls (8.5 meV). The advantage of the new $(C_{BC})_3$ model over the previously proposed $(C_2)_{Si}$ -ls model is more apparent in 4H-SiC, where the latter defect produces only eight LVMs above the bulk spectrum instead of the 10 LVMs observed experimentally.⁷ In contrast, $(C_{BC})_3$ can produce 10 LVMs by combining modes from cubic and hexagonal configurations of the defect. As shown in Fig. 3(b), the LVMs of $(C_{BC})_3$ are also in very good quantitative agreement with experimental values for the D_{II} center (r.m.s. error of 2.6 meV). In addition, since $(C_{BC})_3$ - k exhibits almost identical LVMs in both 3C- and 4H-SiC, it can be the origin of the five “universal” D_{II} phonon modes observed throughout the different polytypes of SiC.

From Table I, the dissociation energy (see Ref. 10 for definition) of $(C_{BC})_3$ is calculated to be 4.36–6.71 eV, depending on the final configuration of the carbon di-interstitial. This value is higher than that of the di-carbon antisite (4.1 eV¹⁰) and is consistent with the observed high thermal stability of the D_{II} center.⁴ In this study, we have further subjected the $(C_{BC})_3$ defect to *ab initio* MD simulations at a very high temperature of 3000 K for a total duration of 15 ps. Simulations are performed in a canonical ensemble with a Nose-Hoover thermostat and a time step of 1 fs. Only the Γ point is used to sample the Brillouin zone, and the plane-wave cutoff energy is reduced to 400 eV. During the time of our simulations, we do not observe any dissociation, reconfiguration, or diffusion of this defect cluster, which provides another line of evidence for the high thermal stability of $(C_{BC})_3$.

IV. CONCLUSIONS

To summarize, using a combination of random configuration sampling, MDs simulated annealing, and first-principles structural refinements, we have discovered a carbon tri-interstitial cluster that is particularly stable in SiC and leads to a distinct minimum of the cluster formation energy (per interstitial). Furthermore, this defect complex exhibits high thermal stability, and the numbers and frequencies of its LVMs match well with the D_{II} PL spectra measured experimentally in 3C- and 4H-SiC. We thus propose that the newly found defect cluster is responsible for the persistent D_{II} center in SiC. Discovery of the nature of the most stable defect clusters in SiC is critical for semiconductor applications of 4H-SiC (as argued in introductory paragraphs), as well as for structural nuclear applications where evolution of radiation-induced defects in 3C-SiC is an active area of research.³⁵

ACKNOWLEDGMENTS

This research is supported by the US Department of Energy, Office of Basic Energy Sciences Grant No. DE-FG02-08ER46493. C.J. also thanks Guangfu Luo of University of Wisconsin for helpful discussions on group theory analysis.

*cjiang32@wisc.edu.

†ddmorgan@wisc.edu.

‡szlufarska@wisc.edu.

- ¹R. Madar, *Nature* **430**, 974 (2004).
- ²J. B. Casady and R. W. Johnson, *Solid-State Electron.* **39**, 1409 (1996).
- ³W. X. Ni, G. V. Hansson, I. A. Buyanova, A. Henry, W. M. Chen, and B. Momemmar, *Appl. Phys. Lett.* **68**, 238 (1996).
- ⁴L. Patrick and W. J. Choyke, *J. Phys. Chem. Solids* **34**, 565 (1973).
- ⁵S. G. Sridhara, D. G. Nizhner, R. P. Devaty, W. J. Choyke, T. Dalibor, G. Pensi, and T. Kimoto, *Mater. Sci. Forum* **264-268**, 493 (1998).
- ⁶F. H. C. Carlsson, S. G. Sridhara, A. Hallen, J. P. Bergman, and E. Janzen, *Mater. Sci. Forum* **433-436**, 345 (2003).
- ⁷W. Sullivan and J. W. Steeds, *Mater. Sci. Forum* **556-557**, 319 (2007).
- ⁸A. Mattausch, M. Bockstedte, and O. Pankratov, *Physica B* **308-310**, 656 (2001).
- ⁹A. Mattausch, M. Bockstedte, and O. Pankratov, *Phys. Rev. B* **69**, 045322 (2004).
- ¹⁰A. Mattausch, M. Bockstedte, and O. Pankratov, *Phys. Rev. B* **70**, 235211 (2004).
- ¹¹A. Gali, P. Deak, P. Ordejon, N. T. Son, E. Janzen, and W. J. Choyke, *Phys. Rev. B* **68**, 125201 (2003).
- ¹²M. Bockstedte, A. Gali, A. Mattausch, O. Pankratov, and J. W. Steeds, *Phys. Status Solidi B* **245**, 1281 (2008).
- ¹³P. Ballone and P. Milani, *Phys. Rev. B* **42**, 3201 (1990).
- ¹⁴R. O. Jones, *Phys. Rev. Lett.* **67**, 224 (1991).
- ¹⁵N. Binggeli, J. L. Martins, and J. R. Chelikowsky, *Phys. Rev. Lett.* **68**, 2956 (1992).
- ¹⁶C. J. Pickard and R. J. Needs, *Phys. Rev. Lett.* **97**, 045504 (2006).
- ¹⁷C. Jiang, Z. J. Lin, and Y. S. Zhao, *Phys. Rev. Lett.* **103**, 185501 (2009).
- ¹⁸G. Lucas, M. Bertolus, and L. Pizzagalli, *J. Phys.: Condens. Matter* **22**, 035802 (2010).
- ¹⁹S. Plimpton, *J. Comp. Phys.* **117**, 1 (1995).
- ²⁰M. Z. Bazant and E. Kaxiras, *Phys. Rev. Lett.* **77**, 4370 (1996).
- ²¹D. A. Richie, J. Kim, S. A. Barr, K. R. A. Hazzard, R. Hennig, and J. W. Wilkins, *Phys. Rev. Lett.* **92**, 045501 (2004).
- ²²S. Lee and G. S. Hwang, *Phys. Rev. B* **77**, 085210 (2008).
- ²³Y. A. Du, T. J. Lenosky, R. G. Hennig, S. Goedecker, and J. W. Wilkins, *Phys. Status Solidi B* **248**, 2050 (2011).
- ²⁴G. Kresse and J. Furthmuller, *Phys. Rev. B* **54**, 11169 (1996).
- ²⁵G. Kresse and D. Joubert, *Phys. Rev. B* **59**, 1758 (1999).
- ²⁶See Supplemental Material at <http://link.aps.org/supplemental/10.1103/PhysRevB.86.144118> for detailed atomic coordinates of the carbon tri-interstitial defect as embedded in a 216-atom cubic SiC supercell.
- ²⁷M. Bockstedte, A. Mattausch, and O. Pankratov, *Phys. Rev. B* **69**, 235202 (2004).
- ²⁸S. B. Zhang and J. E. Northrup, *Phys. Rev. Lett.* **67**, 2339 (1991).
- ²⁹T. Mattila and R. M. Nieminen, *Phys. Rev. B* **54**, 16676 (2006).
- ³⁰J. Heyd, G. E. Scuseria, and M. Ernzerhof, *J. Chem. Phys.* **124**, 219906 (2006).
- ³¹M. Leslie and M. J. Gillan, *J. Phys. C* **18**, 973 (1985).
- ³²D. Shrader, S. M. Khalil, T. Gerczak, T. R. Allen, A. J. Heim, I. Szlufarska, and D. Morgan, *J. Nucl. Mater.* **408**, 257 (2011).
- ³³N. E. B. Cowern, G. Mannino, P. A. Stolk, F. Roozeboom, H. G. A. Huizing, J. G. M. van Berkum, F. Cristiano, A. Claverie, and M. Jaraiz, *Phys. Rev. Lett.* **82**, 4460 (1999).
- ³⁴J. P. Perdew, K. Burke, and M. Ernzerhof, *Phys. Rev. Lett.* **77**, 3865 (1996).
- ³⁵Y. Katoh, L. L. Snead, I. Szlufarska, and W. J. Weber, *Curr. Opin. Solid State Mater. Sci.* **16**, 143 (2012).